ELSEVIER

Marine Geology 180 (2002) 105–116

MARINE GEOLOGY
INTERNATIONAL JOURNAL OF MARINE GEOLOGY, GEOCHEMISTRY AND GEOPHYSICS

www.elsevier.com/locate/margeo

The early Matuyama Diatom Maximum off SW Africa: a conceptual model

W.H. Berger *, C.B. Lange, M.E. Pérez

Scripps Institution of Oceanography, University of California, San Diego, 9500 Gilman Drive, La Jolla, CA 92093-0244, USA

Received 1 July 2000; received in revised form 15 March 2001; accepted 25 May 2001

Abstract

An important discovery during Ocean Drilling Program Leg 175, when investigating the record of upwelling off Namibia, was the finding of a distinct Late Pliocene diatom maximum spanning the lower half of the Matuyama reversed polarity chron (MDM, Matuyama Diatom Maximum) and centered around 2.6–2.0 Ma. This maximum was observed at all sites off southwestern Africa between 20°S and 30°S, and is most strongly represented in sediments of Site 1084, off Lüderitz, Namibia. The MDM is characterized by high biogenic opal content, high numbers of diatom valves, and a diatom flora rich in Southern Ocean representatives (with *Thalassiothrix antarctica* forming diatom mats) as well as coastal upwelling components. Before MDM time, diatoms are rare until ca. 3.6 Ma. After the MDM, in the Pleistocene, the composition of the diatom flora points to increased importance of coastal upwelling toward the present, but is accompanied by a general decrease in opal and diatom deposition. Here we present a simple conceptual model as a first step in formalizing a possible forcing mechanism responsible for the record of opal deposition in the upwelling system off Namibia. The model takes into account Southern Ocean oceanography, and a link with deepwater circulation and deepwater nutrient chemistry which, in turn, are coupled to the evolution of North Atlantic Deep Water (NADW). The model proposes that between the MDM and the Mid-Pleistocene climate revolution, opal deposition off Namibia is not directly tied to glacial–interglacial fluctuations (as seen in the global $\delta^{18}O$ record), but that, instead, a strong deepwater link exists with increased NADW production (as seen in the deepwater $\delta^{13}C$ record) accounting for higher supply of silicate to the thermocline waters that feed the upwelling process. The opal record of Site 1084 shows affinity to eccentricity on the 400-kyr scale but not for the 100-kyr scale. This points toward long-term geologic processes for delivery of silica to the ocean.

Keywords: marine silicate budget; diatom mats; Neogene upwelling; Namibian upwelling system; Walvis Paradox; Matuyama Diatom Maximum; Benguela Current

"...from the irritation which suspense occasions, is the mind forced on to pronounce, without sufficient data for pronouncing."

Cardinal John Henry Newman (1801–1890)

1. Introduction: Paradox of the Matuyama Diatom Maximum

In a previous paper on the early Matuyama Diatom Maximum (MDM) off southwestern Afri-

* Corresponding author. Fax: +1-858-822-3310. *E-mail address:* wberger@ucsd.edu (W.H. Berger).

0025-3227/02/$ – see front matter
PII: S0025-3227(01)00208-0

ca, Lange et al. (1999) summarized the evidence for a distinct diatom maximum within the latest Pliocene, spanning the lower half of the Matuyama reversed polarity chron. This prolonged maximum is centered around 2.6–2.0 Ma, and follows a rapid increase of diatom deposition near 3.1 Ma (Berger et al., 1998).

The evidence for this phenomenon was gathered during the second half of Ocean Drilling Program Leg 175, when the JOIDES Resolution occupied five sites off SW Africa in order to retrieve the record of the Namibia upwelling system (Wefer et al., 1998; see Fig. 1). All of the five sites showed a maximum content of diatom debris beginning in the middle of the Gauss Chron and lasting to just before the Olduvai Chron. At least three sites (1082, 1083, 1084) contain diatom mats of the kind reported from the eastern equatorial Pacific for the latest Miocene and earliest Pliocene (Kemp and Baldauf, 1993), and Sites 1081 and 1085 also show *Thalassiothrix* valves forming an interlocking meshwork. Within the resolution of shipboard stratigraphy, the period of maximum diatom deposition seems to be synchronous. The peak occurs within 100 kyr of 2.2 Ma, in the latest Pliocene, which is somewhat younger than the center of the overall range of the maximum (2.6–2.0 Ma).

Maximum diatom deposition at the end of the Pliocene was earlier reported from Site 532 on Walvis Ridge, together with data on organic carbon and carbonate deposition (Gardner et al., 1984; Hay et al., 1984; Dean and Gardner, 1985; Diester-Haass et al., 1992; Sancetta et al., 1992; Hay and Brock, 1992). In Site 532, as is true for Sites 1081–1085, there is no indication for increased organic matter deposition during the time of the MDM. Paradoxically, organic carbon deposition tends to increase while diatom deposition decreases, after the MDM. Bacterial decay of organic matter may contribute to this difference in trends. However, the discrepancy points to a more fundamental conundrum, that is, that opal deposition is somehow decoupled from the deposition of organic matter. This is also suggested by the 'Walvis Paradox' (Berger and Wefer, 1996), which arises from the observation that opal deposition is decreased during glacial periods (Diester-Haass, 1985; Diester-Haass et al., 1992) while the intensity of upwelling appears to be increased (Oberhänsli, 1991), at least during the late Quaternary.

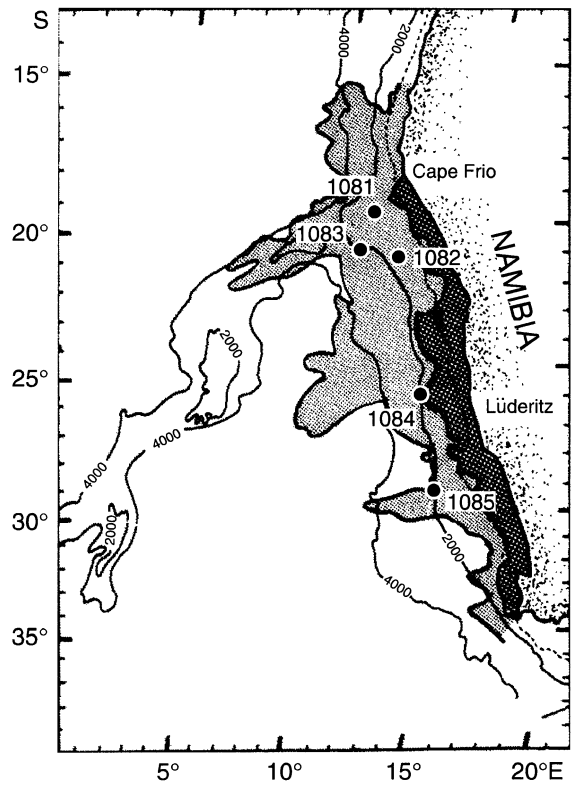

Fig. 1. Location of the Leg 175 sites off southwestern Africa that show the MDM centered between 2.6 and 2.0 Ma. Site 1084 off Lüderitz Bay has the highest opal contents and shows the presence of diatom mats rich in *Thalassiothrix* within the MDM. Heavy shading, coastal upwelling zone; light shading, zone influenced by eddies and filaments from the upwelling zone, as seen in satellite images. From Lange et al. (1999).

Identification of the diatom remains on board the drilling vessel (Shipboard Scientific Party, 1998a) and subsequently on shore (Lange et al., 1999) established that the diatom flora of the MDM has strong antarctic/subantarctic affinities. Intervals rich in the needle-shaped species *Thalassiothrix antarctica* alternate with intervals dominated by upwelling indicators such as *Chaetoceros radicans* and *C. cinctus* (mainly represented as spores and setae), as well as unfragmented *T. nitz-*

schoides. In addition to the strong Southern Ocean and upwelling components, the MDM diatom flora includes nearshore forms and representatives of oligotrophic, warm waters. After the MDM, the floral aspect shifts to dominance of a coastal upwelling influence, as suggested by the constant presence of *Chaetoceros* resting spores (Lange et al., 1999). The record shows a lack of diatom mats, scarcity of Southern Ocean representatives, and increased concentrations of organic matter.

The paradox of the MDM is that increased coastal upwelling in the Pleistocene is accompanied by an apparent decrease in total diatom deposition. The relative increase in coastal upwelling as a source of diatom debris is clear from the preponderance of *Chaetoceros* spores after the MDM. While an increase in upwelling in absolute terms does not necessarily follow from this observation, it is highly probable based on other evidence. Thus, Oberhänsli (1991) has shown quite convincingly that glacial conditions in the late Quaternary are associated with increased coastal upwelling on the Walvis Ridge. The same relationship has now been found for Site 1085, in the early Quaternary (Anderson et al., 2001). Thus, as the glacial component of climate becomes increasingly dominant, after 2 Ma, we should expect an overall increase in coastal upwelling, as a general trend within the Quaternary. In contrast, a decrease in total diatom deposition is readily evident from concentration measurements, either visually (diatom abundance index, DAI) or by determination of opal content (Wefer et al., 1998; Lange et al., 1999; Pérez et al., 2001). It persists when taking into account mass accumulation rates (Lange et al., 1999).

A number of possible explanations have been put forward regarding the origin of the MDM, including a change in silicate content of thermocline waters (Berger et al., 1998; Lange et al., 1999). Here we explore the structure of the problem, that is, we search for the simplest possible description of the phenomenon to be explained. The approach is designed to result in a statement about the minimum number of elements in the system which call for explication.

2. Data base: The opal record of Site 1084

The strongest representation of the MDM is in Site 1084 (25°30′S, 13°01′E; water depth: 1992 m, penetration: 605 mbsf, earliest Pliocene). This is the site where the fundamental difference between the frontal zone assemblage of the MDM (with its diatom mats) and the coastal upwelling assemblage of the Pleistocene (without diatom mats) was first documented in some detail (Shipboard Scientific Party, 1998b). We use the information on diatom abundance and opal percentage in this site, as published in the Appendix of Lange et al. (1999), for the data base of the analysis which follows (Fig. 2). Ages were calculated from shipboard tie points (nannofossil data and paleomagnetic reversals) after transfer into the composite depth frame. Connections between tie points were made by smoothed interpolation of sedimentation rates (rather than by assuming constant sedimentation rate between tie points).

The MDM, with its frontal zone aspects, as described, is seen to be centered between 2.6 and 2.0 Ma, as mentioned (Fig. 2A, DAI). The opal index (opi; log of ratio of opal over non-opal) is similarly centered on this interval; however, it shows an overall increase of opal toward younger ages within the MDM – something that the visual index (DAI) is unable to show, because it has an upper limit at the point where diatom debris is the dominant sediment. The ramping up of opal deposition begins a million years before the MDM is reached; that is, near 3.6 Ma. An abrupt drop to lower values occurs after the MDM, at 2.0 Ma or slightly earlier. After this event, there is a general decrease of opal deposition, marked by increasing amplitudes of fluctuation. In other words, while low-diatom intervals become more prominent in abundance and duration, high-diatom intervals still occur as well, and provide large contrast.

The overall trends are reflected in greatly smoothed versions of the diatom and opal abundance series (Fig. 2B). 'Frontal zone' marks the position of the MDM, with its *Thalassiothrix* diatom mats and rich admixture of Southern Ocean species. The relative importance of 'coastal upwelling' increases toward the present, as documented by *Chaetoceros* resting spores (Lange et

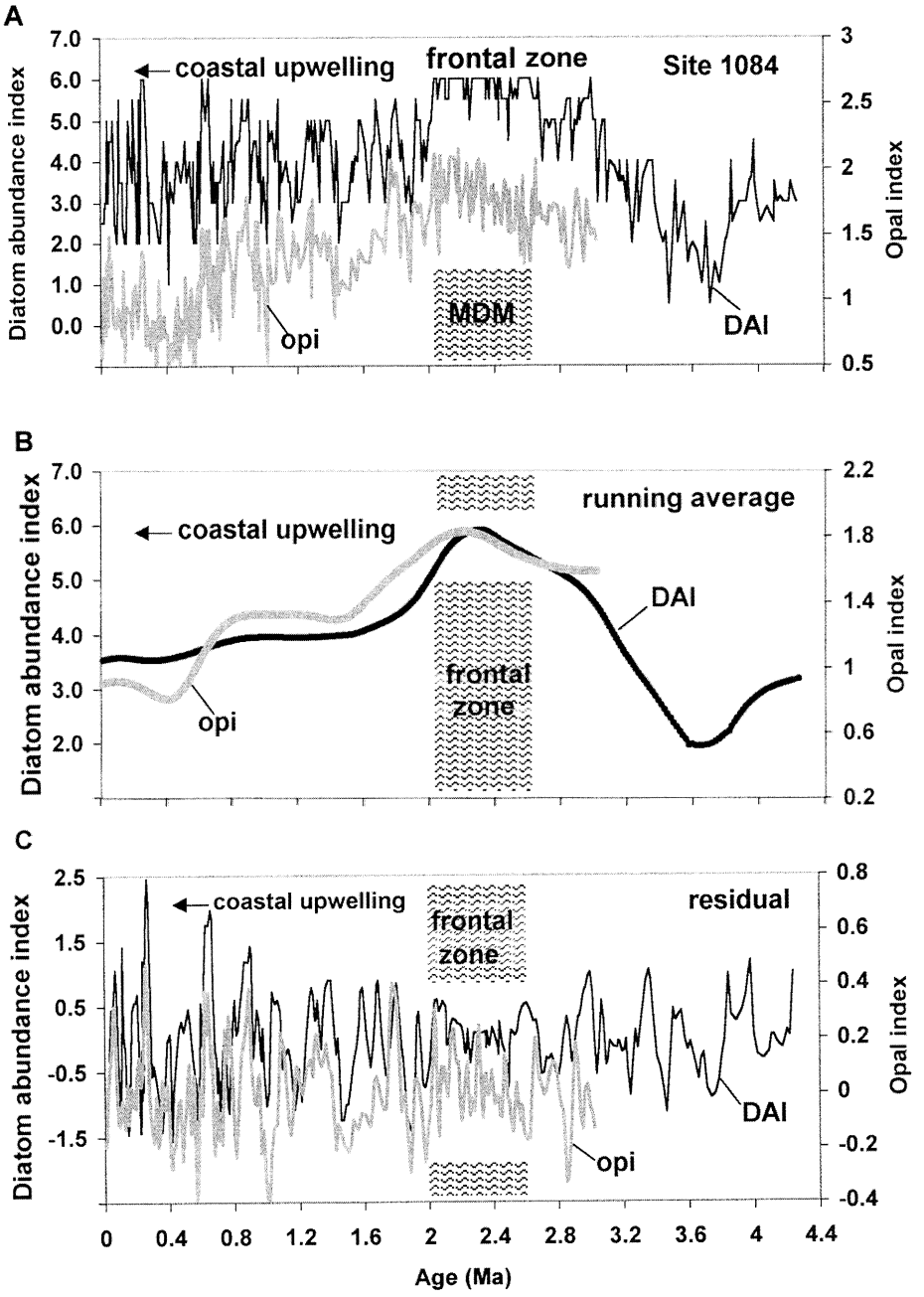

Fig. 2. Diatom and opal deposition in Site 1084 (Hole A). (A) Summary of raw data. DAI, diatom abundance index; opi, opal index; MDM, early Matuyama Diatom Maximum. The opal index is the logarithm of the ratio of opal to non-opal content in the sample measured. Data from Lange et al. (1999). (B) Greatly smoothed versions of the series in the upper panel. DAI and opi as above. 'Frontal zone' marks the position of the MDM. The relative importance of coastal upwelling increases toward the present, as documented by *Chaetoceros* resting spores. At the same time, overall diatom deposition decreases. Note the relative insensitivity of the visual index (DAI) compared to opal %, at low values of opal. (C) Residual values of DAI and opi, after removal of smoothed series from original series. Note the increase of variability in the late Quaternary.

al., 1999). At the same time, overall diatom deposition decreases. The trend toward increasing values within the MDM is now obvious for both indices. For the same amount of smoothing, the opal index tends to show more structure, presumably because of its greater sensitivity; this is especially obvious at low diatom abundance, in the late Quaternary. Removal of the long-term trends results in residual series for both the DAI and the opi (Fig. 2C). Smoothing was performed by repeated application of a 111 boxcar, which is equivalent to diffusion. The process was arbitrarily stopped when the result had the morphology shown in Fig. 2B. The excellent correlation between the two indices is noteworthy, although there is some disagreement in places (near 0.5 Ma and near 1.6 Ma).

In large part, we think, disagreements between the two indices stem from the fact that different samples were analyzed along a rather variable record. Typical sample spacing is shown in Table 1. Thus, by chance, one sampling pattern can land on a series of peaks while another will retrieve a series of lows, on the scale of precession, say. It is evident, from this sample spacing, that a search for cycles at periods of less than 60 kyr in length would be fraught with problems. We have not attempted a search for obliquity periods or shorter periods, therefore.

Encouraged by the good fit of the two indices (Fig. 2C), we have merged the two series in order to decrease sample spacing for better resolution. Considering the differences in sensitivity, especially at the ends of the range of diatom abundance, we have avoided overall linear regression in making the match. Instead, we formed means

Table 1
Sample spacing of the diatom abundance index (DAI) and the opal index (opi) at Site 1084

Age span (Ma)	Diatoms (DAI) (kyr)	Opal (opi) (kyr)
0–0.5	2–25	3–18
0.5–1.0	2–20	3–25
1.0–1.5	5–35	10–40
1.5–2.0	10–35	10–40
2.0–2.5	2–18	8–15
2.5–3.0	10–30	12–20

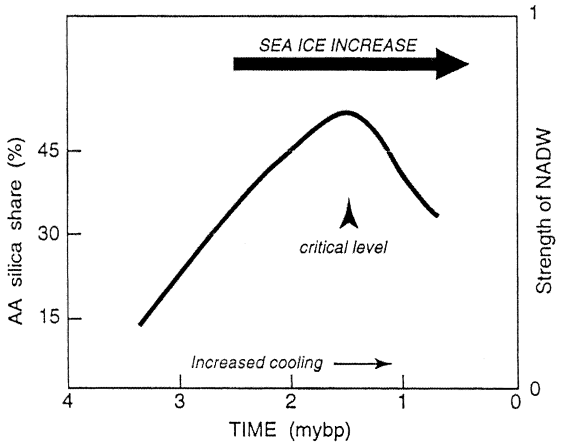

Fig. 3. Hypothesis of early Pleistocene opal maximum in the Southern Ocean, based on the concept of a link to an optimum in NADW production (at the critical level of cooling). From Berger and Wefer (1991).

and standard deviations along each series, using a moving 400-kyr window. We then set the DAI values to the means and standard deviations of the opi values, at the center of the gliding window (this corresponds to local linear regression). Finally, we merged the DAI transforms with the opi values, according to assigned age (by simple sorting). The merged series was smoothed with a 121 filter simultaneously for both age and index, and then interpolated for 8-kyr intervals. This new series is labeled 'opx' and will be used for time series analysis.

3. Hypothesis: Concept of optimum

The smoothed version of opal deposition shows a ramp-up beginning between 4 and 3 Ma, a maximum centered near 2.3 and 2.2 Ma and a subsequent decline (Fig. 2B). The overall trend is reminiscent of the proposition that the share of opal deposition around Antarctica (of total global deposition) moves through an optimum as the planet cools (Fig. 3). The reason given is that an overall increase in the production of North Atlantic Deep Water (NADW), due to cooling in the late Pliocene, will move silicate into the Southern Ocean, increasing diatom production there (Berger and Wefer, 1991). This proposed mechanism is re-

ferred to as the 'fire-hose effect' (Boyle and Rosenthal, 1996). At some critical level, additional cooling interferes with NADW production (for example through sea ice formation, or from decreased export of water vapor from the North Atlantic), negatively impacting the 'fire-hose' effect. At that point, diatom production in the Southern Ocean decreases and the Antarctic Ocean's share in the global ocean silica sequestration drops. The concept of an early Pleistocene Antarctic opal silica optimum has recently been supported by the results of Leg 177, in a south–north transect from Bouvet Island to Agulhas Ridge south of the Cape (Gersonde et al., 1999). *Thalassiothrix* diatom mats are reported from Site 1091 (47°S) in the early Pleistocene, and also in Site 1093 (50°S).

Can we link these propositions and findings to the upwelling regime off SW Africa? To do this, one would need to show that the formation of thermocline waters (which feed the upwelling) is tied rather closely to the oceanography of the Southern Ocean. The formation of thermocline waters in the South Atlantic is a complicated process and is the subject of intense study (Talley, 1996). It is reasonable to suppose, however, that the silicate content of these subducted waters will be strongly influenced by the proximity of newly upwelled Southern Ocean waters to the location of convergence, and by the richness of these deep waters as concerns the silicate content. Both factors, presumably, will depend not only on general conditions (such as planetary temperature gradient and associated wind fields) but also on the specific process of silicate supply from northern deep waters. We reason, therefore, that a strong supply of NADW waters will be favorable to high silicate values in thermocline waters: the band of vertical convection in the Southern Ocean will be wide (bringing frontal action northward into the range of interaction with the Benguela system) and the silicate content will be high (through the 'fire-hose' effect).

The lag of the Antarctic diatom maximum (early Quaternary) with respect to the Namibian diatom maximum (latest Pliocene) would seem to indicate an increased separation of the Antarctic ring of deep vertical mixing from the convergence where thermocline waters are subducted in the subantarctic regions. We suggest that this separation is a result of spin-up and contraction of the Circumpolar Current.

The concept of optimum conditions (whatever the details) suggests an approach whereby we analyze the data in terms of distance from the optimum, on a general cooling trend. The concept of the influence of NADW production suggests investigating deepwater chemistry as a possible factor in driving opal deposition off SW Africa. To these two tasks we turn next.

4. Model: Overall cooling and distance from optimum

For a conceptual modeling of opal deposition we use two driving factors: global system state and distance from optimum condition. For the target, we use the smoothed DAI series (Fig. 2B), which reaches back before 4 Ma. The global system state (that is, a measure of the condition of the planet in terms of overall temperature gradients, wind fields, intensity of upwelling, deep circulation) could be expressed in a number of ways; we use the smoothed series of $\delta^{18}O$ of deepwater benthic foraminifers in the deep Pacific (Site 849, Mix et al., 1995). Along this line (Fig. 4A, 'system state'), we mark off a range for optimal conditions, between 3.5 and 3.65 on the oxygen isotope index, corresponding to the time span from 2.8 and 2.1 Ma ('frontal zone optimum', Fig. 4A, note intersection with 'system state'). The algorithm that translates system state and distance from optimum into an estimate of diatom deposition has the form of a linear regression:

$$Dx = a \times \{f(\text{dist})\} + b \times \delta^{18}O + c \quad (1)$$

where f(dist) is the inverse of the difference of the given state (x) to the nearest point on the optimum (fz), augmented by 0.5 (to avoid dividing by zero):

$$f(\text{dist}) = 1/(|(x - fz)| + 0.5) \quad (2)$$

The coefficients a and b and the constant c are

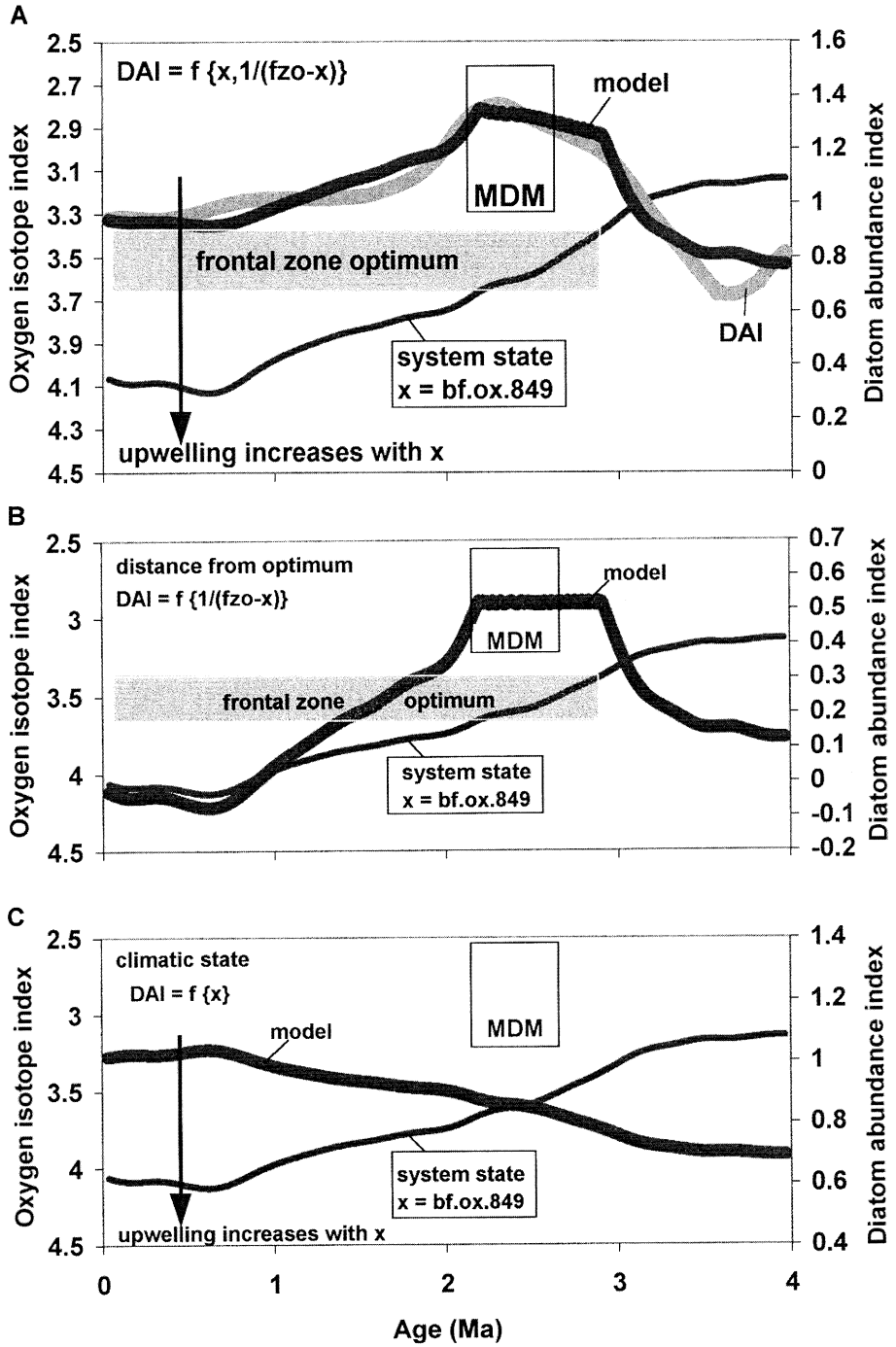

Fig. 4. Conceptual model of the record of opal deposition off SW Africa, in the last 4 million years. (A) Target (DAI, smoothed, from Fig. 2B), elements of the model ('system state', 'frontal zone optimum'), algorithm (DAI=$f\{x,1/(fzo-x)\}$) and output ('model'). The system state is the $\delta^{18}O$ of benthic foraminifers in Site 849, in the eastern equatorial Pacific (Mix et al., 1995); it is 'x' in the algorithm. The term '$fzo-x$' is the distance to the closest point in the frontal zone optimum (see text for details). (B) Model generated using the first term of the algorithm only. (C) Model generated using the second term of the algorithm only.

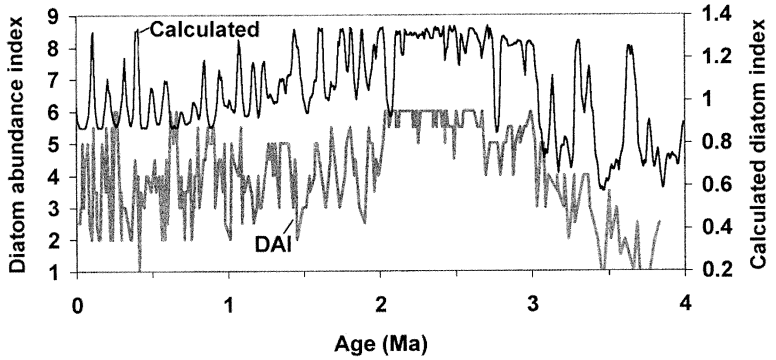

Fig. 5. Performance of the algorithm (Eq. 1) for modeling short-term fluctuations of opal deposition. Input is unsmoothed (original) $\delta^{18}O$ series of Site 849 (benthic foraminifers, Mix et al., 1995).

adjusted for best fit. In Fig. 4A, the term $(|(x-fz)|+0.5)$ is written as $(fzo-x)$ for brevity. The series resulting from applying the algorithm to the $\delta^{18}O$ series as drawn reflects the target quite well (Fig. 4A). To illustrate the meaning of the two terms in the algorithm (Eq. 1), we run the terms separately. The term reflecting distance from the optimum $\{f(1/(fzo-x)\}$ produces a mesa-like structure, which yields a maximum and rapid drop-off next to it, but fails to represent the overall difference before and after the maximum (Fig. 4B). The term reflecting the changing system state (overall cooling, intensity of upwelling, $\{f(x)\}$) produces a model which is a simple mirror image of the $\delta^{18}O$ input series (Fig. 4C). Together, the two terms produce the observed fit, with opal deposition being considerably higher after the MDM than before it. Also, by tilting the mesa top maximum produced by the first term (Fig. 4B), the second term shifts the maximum closer to the termination of optimum conditions, as observed.

How well does the algorithm (Eq. 1) perform when asked to reproduce not just the smooth version of the diatom abundance (for which it was fitted), but the higher-frequency fluctuations in diatom and opal content? To answer this question, we use the original $\delta^{18}O$ series from Site 849 as input, rather than the smoothed series (as in Fig. 4). Results of the test compare well with the overall structure of the DAI record, reproducing a sense of the overall variability in pre-MDM and post-MDM which is quite in line with what is observed (Fig. 5). However, in detail results are disappointing: the predicted peaks and valleys do not match the observed ones. The mismatch on the scale of 100 kyr could be due to dating problems. There is no reason to expect that the shipboard age model is precise on this scale (while that of Site 849 is orbitally tuned). Alternatively, the simple model proposed (relying on $\delta^{18}O$ and distance of $\delta^{18}O$ values from optimum conditions) is inappropriate for describing opal fluctuations at the 100-kyr scale.

5. A search for forcing: Deepwater link and Milankovitch

If $\delta^{18}O$ is unable to describe the conditions of opal deposition, might there be other factors to be considered? To deal with this question we return to the second part of the working hypothesis about an Antarctic silica optimum (Fig. 3), that is, to the link with deepwater circulation. The nutrient chemistry of the deep waters of the ocean is linked through global exchange processes, with the production of NADW playing a major role in modifying that chemistry (Keir, 1988; Raymo et al., 1997). An excellent marker for the oxygen and nutrient content of deep waters is the $\delta^{13}C$ composition of benthic foraminifers (Wefer and Berger, 1991). Thus, if deepwater chemistry is important in the opal record off SW Africa, and if it is tied to NADW production, we should expect a correlation between the Pacific deepwater $\delta^{13}C$

and the rate of opal deposition in the Benguela Current.

Such a correlation appears to exist (Fig. 6). Also, it has the correct sign for the expectation that increased NADW production (which lowers the $\delta^{13}C$ values in Pacific deep waters) increases opal deposition in the southern South Atlantic. Previous to the onset of 100-kyr cycles (near 700 kyr, Berger and Wefer, 1992; Mudelsee and Stattegger, 1997), there is a remarkable similarity between the opal abundance in Site 1084 ('opx') and the $\delta^{13}C$ record of benthic foraminifers in Site 849, in the deep Pacific ('C-13', Mix et al., 1995). However, within the last 600 kyr (Milankovitch Chron, characterized by large climate excursions) a correlation is not obvious. The match over much of the Quaternary (excepting the last third) suggests that the concept of a deepwater link is correct. Its deterioration in the late Pleistocene indicates a regime shift, such that late Quaternary mechanisms cannot be easily invoked to explain variations for the rest of post-MDM time.

The $\delta^{13}C$ signal (from Site 849) is not entirely independent from the $\delta^{18}O$ signal. We might ask, therefore, whether variation in $\delta^{18}O$ indirectly influences opal deposition, by way of the $\delta^{13}C$ variation. Interestingly, if the portion of the $\delta^{13}C$ that is correlated to $\delta^{18}O$ in the record of Site 849 is removed from the $\delta^{13}C$ record (by calculating $\delta^{13}C$ from regression on $\delta^{18}O$ and taking the difference to the observed $\delta^{13}C$), the match with the opal record is improved for pre-Milankovitch time, but is worsened for the Milankovitch Chron (last 625 kyr). This exercise would seem to suggest that glacial–interglacial cycles (as recorded by $\delta^{18}O$) are less important than deep circulation (as seen in $\delta^{13}C$) in the early two thirds of post-MDM time, for the opal record, but gain importance for the last third, when they attain a dominant role in climate change.

In the introductory essay to the present volume, the point is made that the opal record of Site 1084 shows affinity to eccentricity (that is, the potential for seasonal contrast) on the 400-kyr scale. It is intriguing to note that no such relationship exists for the 100-kyr scale (Fig. 7). The correlation between eccentricity and opal abundance is zero, both for the early and for the late Quaternary. Given the fact that the 100-kyr ice-age cycle dominates climate in the late Quaternary, and that it is clearly tied to eccentricity (through amplitude modification of the precessional effect, emphasized by Milankovitch, 1930), it is surely surprising to note this lack of response displayed in the opal record.

The fact that the 400-kyr cycle is represented in the opal record, while the 100-kyr cycle is not, would seem to point toward processes that have to do with long-term cyclic geologic processes, such as the intensity of weathering of silicate minerals on land, with associated changes in supply of silica by rivers. Large long-period changes in seasonal contrast – which prevent attainment of equilibrium, a state with reduced reaction rates –

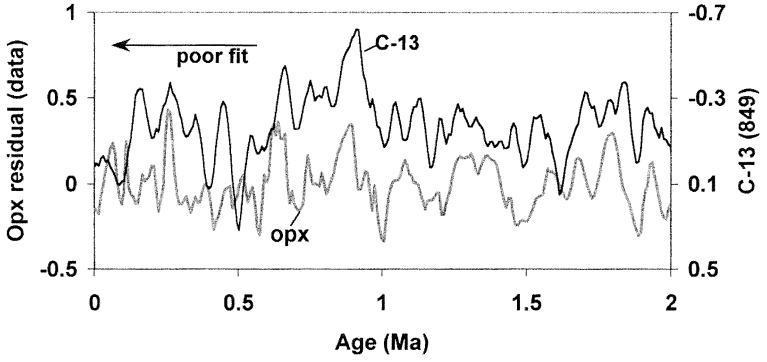

Fig. 6. The link between the Namibia opal record and global ocean deepwater nutrient chemistry, as seen in the relationships between opal abundance ('opx') and carbon isotope composition of Pacific deep water (Site 849, Mix et al., 1995). Note reversed scale for $\delta^{13}C$. The correlation over the entire 2 Ma is significant at $P < 0.01$, but is comparatively poor in the last third of the record.

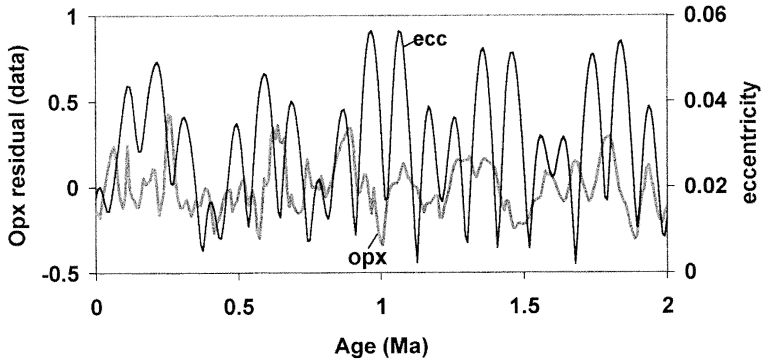

Fig. 7. Relationship of opal record of Site 1084 to eccentricity of the Earth's orbit (Berger and Loutre, 1991).

presumably are ideal for optimal delivery of silica to the ocean.

The presence of cycles in the opal record at periods below 400 kyr and above 60 kyr is further checked by calculating an evolutionary spectrum with a window of 800 kyr and an offset of 400 kyr. Nine spectra were calculated using autocorrelation and standard Fourier expansion. The merged residual opal record (opx) was used for the last 3 million years, and the equivalent DAI record for the time before that, back to 4.4 Ma (Fig. 8). The output was corrected for a general trend by dividing Fourier amplitudes by the square of log (period). This subdues amplitudes to the left (long periods) and enhances those to the right of the graph (short periods).

The overall average of the spectra (top of graph) shows maximum power near 240 kyr, a secondary peak near 130 kyr, and a minor peak near 77 kyr. The peak near 130 kyr can be readily assigned to the eccentricity period near 125 kyr, given the broadness of the maximum. This period represents the maximum cyclicity for the intervals centered on 2 Ma (end of MDM) and also on 0.4 Ma (that is, the Brunhes chron). The periods of 77 kyr and 240 kyr are close to a whole-fraction relationship (1 to 3); one tends to be strong where the other is weak, and vice versa. In addition, the 240-kyr period is close to twice the eccentricity line at 125 kyr. What needs explanation, then, is the presence of the 77-kyr period, which has no obvious parent. We note that the sum tone of 413 (main eccentricity period) and 95 (second most important eccentricity period) is 77 kyr and we propose, therefore, that this period is related to eccentricity.

The lack of consistency in periodicity is perhaps the most striking property of the spectral landscape of the opal record of Site 1084. Additional

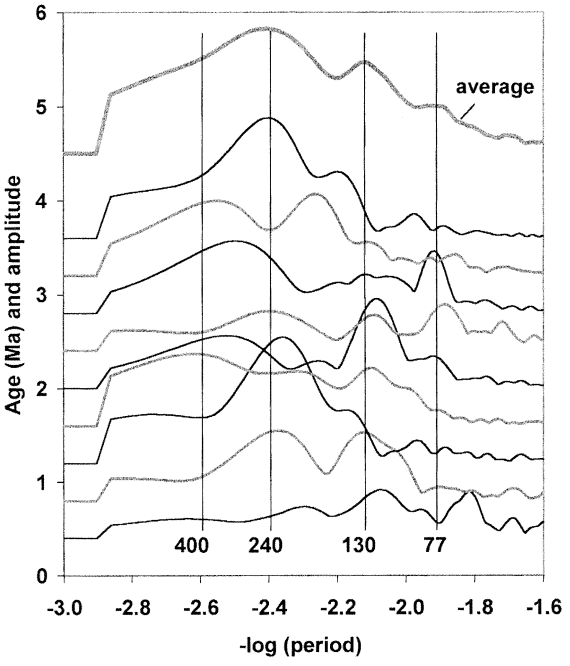

Fig. 8. Evolutionary spectrum of opal record (opx for last 3 Ma, DAI only before that). Fourier expansion of autocorrelation series is used to determine amplitude, which was modified by dividing each entry by the log (period) squared.

work, on other sites, will have to verify whether this is a general property of the Namibia opal record. If so, it would suggest that the various factors responsible for producing the opal record constantly change their interactions as the boundary conditions change. Some of these changes are of a purely geographic nature, such as the closure of the Panama Isthmus (Keller et al., 1989; Coates et al., 1992) which had a profound influence on deepwater production (Keigwin, 1982; Maier-Reimer et al., 1990). Others involve the changing imbalance between the cold South and the relatively warm North (Flohn, 1984), especially in the Atlantic realm. Yet others revolve around the continued build-up of maximum ice masses in the northern hemisphere, culminating in the Mid-Pleistocene climate revolution, and shortly after moving the system into the familiar 100-kyr ice-age cycles.

The appearance of the spectral landscape of the opal record (Fig. 8) suggests that it will be difficult to find simple rules leading from the physical state of the system (and Milankovitch forcing) to the output observed; that is, the production and deposition of diatoms off SW Africa. In a global context, finding the links between the diatom production in eastern boundary upwelling and the changes in opal production in the Antarctic Ocean, as the planet cools (Baldauf and Barron, 1990), is of prime importance for advancing the understanding of the Neogene history of ocean productivity.

Acknowledgements

We thank the Shipboard Scientific Party and ODP staff for their efforts in securing the materials which are the basis for this study. We are grateful to J. Giraudeau for the nannofossil stratigraphy, to T. Yamazaki and G.M. Frost for the magnetostratigraphy, and to V. Spiess and B. Laser for the composite depth determination. We also acknowledge Hui-Ling Lin for providing Site 1084 opal data. This study was supported by JOI/USSSP Grant 418925-BA107 to W.H.B. M.E.P. acknowledges support from the Basque Country Government.

References

Anderson, P.A., Charles, C.D., Berger, W.H., 2001. Productivity fluctuations off southwestern Africa in the early Quaternary, ODP Site 1085. Proc. ODP, Scientific Results, 175. Ocean Drilling Program, College Station, TX.

Baldauf, J.G., Barron, J.A., 1990. Evolution of biosiliceous sedimentation patterns – Eocene through Quaternary: paleoceanographic response to polar cooling. In: Bleil, U., Thiede, J. (Eds.), The Geological History of Cenozoic Polar Oceans: Arctic Versus Antarctic. Kluwer Academic, Dordrecht, pp. 575–607.

Berger, A., Loutre, M.F., 1991. Insolation values for the climate of the last 10 million years. Quat. Sci. Rev. 10, 297–317.

Berger, W.H., Wefer, G., 1991. Productivity of the glacial ocean: Discussion of the iron hypothesis. Limnol. Oceanogr. 36, 1899–1918.

Berger, W.H., Wefer, G., 1992. Klimageschichte aus Tiefseesedimenten – Neues vom Ontong Java Plateau (Westpazifik). Naturwissenschaften 79, 541–550.

Berger, W.H., Wefer, G., 1996. Expeditions into the past: Paleoceanographic studies in the South Atlantic. In: Wefer, G., Berger, W.H., Siedler, G., Webb, D.J. (Eds.), The South Atlantic: Present and Past Circulation. Springer-Verlag, Berlin, pp. 363–410.

Berger, W.H., Wefer, G., Richter, C., Lange, C.B., Giraudeau, J., Hermelin, O., Shipboard Scientific Party, 1998. The Angola-Benguela upwelling system: paleoceanographic synthesis of shipboard results from Leg 175. In: Wefer, G., Berger, W. H., and Richter, C. et al. (Eds.), Proc. ODP, Initial Reports, 175. Ocean Drilling Program, College Station, TX, pp. 505–532.

Boyle, E., Rosenthal, Y., 1996. Chemical hydrography of the South Atlantic during the last Glacial Maximum: Cd vs. $\delta^{13}C$. In: Wefer, G., Berger, W.H., Siedler, G., Webb, D.J. (Eds.), The South Atlantic: Present and Past Circulation. Springer-Verlag, Berlin, pp. 423–443.

Coates, A.G., Jackson, J.C., Collins, L.S., Cronin, T.M., Dowsett, H.J., Bybell, L.M., Jung, P., Obando, J.A., 1992. Closure of the Isthmus of Panama: The near-shore marine record of Costa Rica and western Panama. Geol. Soc. Am. Bull. 104, 814–828.

Dean, W., Gardner, J., 1985. Cyclic variations in calcium carbonate and organic carbon in Miocene to Holocene sediments, Walvis Ridge, South Atlantic Ocean. In: Hsü, K.J., Weissert, H.J. (Eds.), South Atlantic Paleoceanography. Cambridge University Press, Cambridge, pp. 61–78.

Diester-Haass, L., 1985. Late Quaternary upwelling history off southwest Africa (DSDP Leg 75, HPC 532). In: Hsü, K.J., Weissert, H.J., (Eds.), South Atlantic Paleoceanography. Cambridge University Press, Cambridge, pp. 47–55.

Diester-Haass, L., Meyers, P.A., Rothe, P., 1992. The Benguela Current and associated upwelling on the southwest African margin: a synthesis of the Neogene-Quaternary sedimentary record at DSDP Sites 362 and 352. In: Summerhayes, C.P., Prell, W.L., Emeis, K.C. (Eds.), Up-

welling Systems: Evolution Since the Early Miocene. Geol. Soc. London Spec. Publ. 64, 331–342.
Flohn, H., 1984. Climatic evolution in the Southern Hemisphere and the equatorial region during the late Cenozoic. In: Vogel, J.C. (Ed.), Late Cainozoic palaeoclimates of the Southern Hemisphere. A.A. Balkema, Rotterdam, pp. 5–20.
Gardner, J.V., Dean, W.E., Wilson, C.R., 1984. Carbonate and organic-carbon cycles and the history of upwelling at Deep Sea Drilling Project Site 532, Walvis Ridge, South Atlantic Ocean. Init. Rep., Deep Sea Drilling Project 75, 905–921.
Gersonde, R., Hodell, D.A., Blum, P. et al., 1999. Proc. ODP, Initial Reports, 177 [CD-ROM]. Ocean Drilling Program, College Station, TX.
Hay, W.W., Brock, J.C., 1992. Temporal variation in intensity of upwelling off Southwest Africa. In: Summerhayes, C.P., Prell, W.L., Emeis, K.C. (Eds.), Upwelling Systems: Evolution Since the Early Miocene. Geol. Soc. London Spec. Publ. 64, 463–497.
Hay, W.W., Sibuet, J.C. et al., 1984. Site 532: Walvis Ridge. Init. Rep., Deep Sea Drilling Project 75, 295–445.
Keigwin, L.D., 1982. Isotope paleoceanography of the Caribbean and east Pacific: role of Panama uplift in late Neogene time. Science 217, 350–353.
Keir, R.S., 1988. On the late Pleistocene ocean geochemistry and circulation. Paleoceanography 3, 413–445.
Keller, G., Zenker, C.E., Stone, S.M., 1989. Late Neogene history of the Pacific-Caribbean gateway. J. South Am. Earth Sci. 21, 73–108.
Kemp, A.E.S., Baldauf, J.G., 1993. Vast Neogene laminated diatom mat deposits from the eastern equatorial Pacific Ocean. Nature 362, 141–144.
Lange, C.B., Berger, W.H., Lin, H.-L., Wefer, G., Shipboard Scientific Party Leg 175, 1999. The early Matuyama Diatom Maximum off SW Africa, Benguela Current System, ODP Leg 175. Mar. Geol. 161, 93–114.
Maier-Reimer, E., Mikolajewicz, U., Crowley, T.J., 1990. Ocean general circulation model sensitivity experiment with an open American Isthmus. Paleoceanography 5, 349–366.
Milankovitch, M., 1930. Mathematische Klimalehre und astronomische Theorie der Klimaschwankungen. Handbuch der Klimatologie, Bd 1, Teil A. Bornträger, Berlin, 176 pp.
Mix, A.C., Pisias, N.G., Rugh, W., Wilson, J., Morey, A., Hagelberg, T.K., 1995. Benthic foraminifer stable isotope record from Site 849 (0–5 Ma): local and global climate changes. In: Pisias, N.G., Mayer, L.A., Janecek, T.R., Palmer-Julson, A., van Andel, T.H. (Eds.), Proc. ODP, Scientific Results, 138. Ocean Drilling Program, College Station, TX, pp. 371–412.
Mudelsee, M., Stattegger, K., 1997. Exploring the structure of the mid-Pleistocene revolution with advanced methods of time-series analysis. Geol. Rundsch. 86, 499–511.
Oberhänsli, H., 1991. Upwelling signals at the northeastern Walvis Ridge during the past 500,000 years. Paleoceanography 6, 53–71.
Pérez, M.E., Lin, H.-L., Lange, C.B., Schneider, R.R., 2001. Plio-Pleistocene opal records off SW Africa, ODP Sites 1082 and 1084. Proc. ODP, Scientific Results, 175. Ocean Drilling Program, College Station, TX.
Raymo, M.E., Oppo, D.W., Curry, W., 1997. The mid-Pleistocene climate transition: A deep sea carbon isotopic perspective. Paleoceanography 12, 546–559.
Sancetta, C.A., Heusser, L., Hall, M.A., 1992. Late Pliocene climate in the Southeast Atlantic; preliminary results from a multi-disciplinary study of DSDP Site 532. Mar. Micropaleontol. 20, 59–75.
Shipboard Scientific Party, 1998a. Site 1084. In: Wefer, G., Berger, W.H., Richter, C. et al. (Eds.), Proc. ODP, Initial Reports, 175. Ocean Drilling Program, College Station, TX, pp. 339–384.
Shipboard Scientific Party, 1998b. Introduction: background, scientific objectives, and principal results for Leg 175 (Benguela Current and Angola-Benguela upwelling systems). In: Wefer, G., Berger, W.H., Richter, C. et al. (Eds.), Proc. ODP, Initial Reports, 175. Ocean Drilling Program, College Station, TX, pp. 7–25.
Talley, L.D., 1996. Antarctic Intermediate Water in the South Atlantic. In: Wefer, G., Berger, W.H., Siedler, G., Webb, D., (Eds.), The South Atlantic: Present and Past Circulation. Springer-Verlag, Heidelberg, pp. 219–238.
Wefer, G., Berger, W.H., 1991. Isotope paleontology: growth and composition of extant calcareous species. Mar. Geol. 100, 207–248.
Wefer, G., Berger, W.H., Richter, C., Shipboard Scientific Party, 1998. Proceedings of the Ocean Drilling Program, Initial Reports, 175 (2 pts.). Ocean Drilling Program, College Station, TX.